Spectral Overlay of Direct-Sequence Spread Spectrum in the Instrument Landing System Glideslope Band

David W. Matolak[*] and Joshua T. Neville[†]
Ohio University, Athens, Ohio 45701

In this paper, we examine the effects of intentional spectral overlay between a direct-sequence spread spectrum (DS-SS) code-division multiple-access (CDMA) system and the glide slope signal of the Instrument Landing System (ILS) currently employed by the Federal Aviation Administration (FAA). The purpose of the overlay system is to enable increased spectral efficiency (higher data throughput), for future potential aeronautical datalink communications, e.g., an "airborne internet." That is, this overlay would enable simultaneous use of the ILS glideslope band by the current glide slope systems and a new DS-SS CDMA digital communication system. We estimate the performance degradation incurred by both systems for several values of transmit powers, DS-SS bandwidths and data rates, and typical ILS glideslope and CDMA system parameters. Our study uses both analysis and computer simulations. We provide examples that explore both ILS glideslope and CDMA system parameter values appropriate for the successful application of the overlay technique.

I. Introduction

THE need for additional communication capabilities in civilian aviation is well documented. To support this claim, one can cite the Federal Aviation Administration's (FAA) National Airspace System (NAS) "modernization blueprint,"[1] any one of numerous papers from recent professional conferences in the field, such as the Digital Avionics Systems Conferences (DASC), e.g., Refs. 2 and 3, or recent Integrated Communications, Navigation, and Surveillance (ICNS) workshops, e.g., Refs. 4 and 5. The growth of passenger communications is also expected.[6] This work is another in the area of feasibility and tradeoff studies aimed at exploring possible methods to provide new aviation communication services.

Additional communication capabilities, along with additional navigation and surveillance capabilities, will require not only new technologies, but careful planning. The aim toward integration of these three functions (hence: ICNS) has initiated many studies on technology options, e.g., Refs. 7 and 8, and many on planning efforts.

Until now, each component of the NAS has traditionally occupied and operated, independently, in its own reserved frequency spectrum. For example, VHF communications is allocated the 118.0-137.0 MHz frequency spectrum; navigation is allocated 108–118 MHz, 329-335 MHz, and parts of the band in the 900-1090 MHz spectrum (e.g., DME covers 978 MHz to 1213 MHz); and some surveillance (secondary radar transponders) is allocated 1030 and 1090 MHz plus guard bands. Next generation Air Traffic Control/Air Traffic Management (ATC/ATM) infrastructure development and systems, such as proposed by the NASA Small Aircraft Transportation System (SATS), are driving toward an "integrated" CNS system solution that can operate in a single "swath" of spectrum to gain efficiency in bandwidth usage and economy from integration of services.

Also, given that current services cannot be eliminated (at least not without a careful transition plan, over a potentially very long time period), additional frequency spectrum allocations appear essential to any successful new

*Assistant Professor, School of Electrical Engineering and Computer Science Avionics Engineering Center, matolak@ohiou.edu.
†Graduate Student, School of Electrical Engineering and Computer Science Avionics Engineering Center, jn40527@ohio.edu.

aviation data link (ADL). This need for datalink bandwidth, beyond the currently used allocations dedicated to existing services, requires that the FAA examine spectrum usage across and beyond the traditional aeronautical spectrum. NASA Glenn Research Center's (GRC) continuing research into advanced communication systems has made significant contributions to the efforts of the FAA to enhance and improve the state of ATC/ATM communications.

This work, in support of NASA Glenn and the FAA, is part of a study to explore innovative approaches to providing new communications services. Our focus here is on the Instrument Landing System (ILS) glideslope band, from 329-335 MHz. Based upon common versions of direct-sequence spread-spectrum (DS-SS) systems, we investigate the use of spectral overlay—the simultaneous use of DS-SS and a narrowband (ILS glideslope) system in the same band.[9] This concept relies on the interference suppression capabilities of DS-SS to enable higher aggregate throughputs than are possible with either a narrowband or DS-SS signaling scheme alone. We note that overlay is in itself something of a worst case, and that via conventional approaches in which different services are allocated orthogonal (non-overlapping) spectral allocations, the performance of both systems is invariably better. Thus, if overlay can be shown to be feasible, orthogonal allocations in the same frequency band are definitely feasible.

We employ classical analytical techniques, corroborated by computer simulation, to characterize the performance of both DS-SS and ILS glideslope systems in the presence of each other. The DS-SS performance is gauged in the usual way for a digital communication system, by bit error probability P_b (or bit error ratio, BER); the ILS glideslope performance is gauged via the signal-to-noise-plus-interference ratio, SNIR. While SNIR may not be the best metric for studying performance of the ILS glideslope navigation system, it is a reasonable initial one, and yields tractable analytical (and computer simulation) results that yield insight into the effects of such an overlay approach. We also note that in recent years, a two-frequency glideslope system has seen widespread deployment.[10] As initial work, our study here addresses only the single frequency system, and we leave study of the two-frequency system for future work.

In Sec. II we describe the system model, assumptions, and introduce notation. The mathematical analysis of performance is in Sec. III, for both systems, and in Sec. IV we provide numerical results—both analytical and simulations. Section V contains a summary.

II.   System and Signal Models

In establishing our model, several assumptions were made. To begin with, the distance between the Instrument Landing System glideslope transmitter and the DS-SS transmitter is assumed to be small in relation to the distance between the aircraft and the runway. We also assume that the ILS glideslope signal is centered on the DS-SS carrier frequency. This is a worst case condition for the DS-SS receiver. In addition, multipath is neglected to simplify analysis. For most applications, the aircraft will have a line of sight to the ground transceivers, hence, our first order model for the channel is an additive white Gaussian noise (AWGN) channel. While this is clearly a simplification, it provides insight into the feasibility of overlay, and allows generation of results to which future studies can compare. In addition, the AWGN channel performance provides a lower bound to the achievable performance in other channel types. Finally, we emphasize that spatial variations of the signal will occur depending upon aircraft orientation and location, but we do not address this for reasons of simplicity—our analysis can thus be considered as applicable to a single point in space/time, a "snapshot" of performance. This can be viewed as a necessary first step in analyzing the more complex case with spatial and time variations.
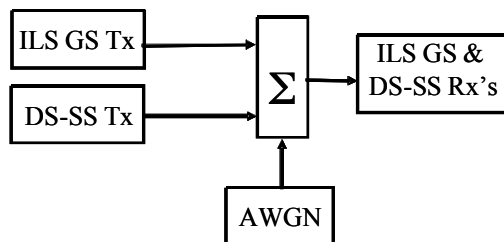

Fig. 1 Conceptual Model of DS-SS overlay system.

Figure 1 shows a conceptual model of our system. We first analyze the performance of the DS-SS signal in the presence of the ILS glideslope signal, then analyze the effect of the DS-SS signal on the ILS glideslope performance. For brevity, we henceforth abbreviate ILS glideslope by simply GS.

The GS signal is an amplitude modulated signal. It consists of five tones: one at the center frequency, and two above and two below the center frequency. The GS signal as seen by the DS-SS receiver can be defined as follows:

$$g(t) = A_c \left[1 + k_a m(t)\right] \cos\left(2\pi f_c t + \phi\right) \tag{1}$$

where A_c is the amplitude of the received signal, k_a is the amplitude modulator constant, f_c is the carrier frequency (329-335 MHz), φ is the carrier signal phase with respect to the DS-SS receiver, and $m(t)$ is the message signal. The worst-case effect on the DS-SS signal is obtained when the GS signal center frequency is equal to the DS-SS carrier frequency,[11] so we analyze this case. Because of the spatial variation of the signal, we also assume that the phase ϕ is equal to zero (this turns out to be a worst-case condition for the DS-SS receiver as well). The analysis parallels the classical one for a single tone jammer in the DS-SS band, e.g., in Ref. 11, but here with multiple tones. The message signal, $m(t)$, is given as follows:

$$m(t) = D \cos\left(2\pi 150 t + \phi_{150}\right) + D \cos\left(2\pi 90 t + \phi_{90}\right) \tag{2}$$

where D is the amplitude of the tones at 150 and 90 Hz from the carrier, and similarly for the phase terms (ϕ's). Equation (2) applies strictly when the receiver is on the GS "centerline," but for simplicity in this initial analysis, we consider only this case as our "snapshot."

We expand $g(t)$ via trigonometric identities to obtain the following form:

$$g(t) = A_c \cos\left(2\pi f_c t\right) + \left(\frac{A_c D k_a}{2}\right)\left[\cos\left(2\pi(f_c + 90)t + \phi_{90}\right) + \cos\left(2\pi(f_c - 90)t - \phi_{90}\right)\right]$$
$$+ \left(\frac{A_c D k_a}{2}\right)\left[\cos\left(2\pi(f_c + 150)t + \phi_{150}\right) + \cos\left(2\pi(f_c - 150)t - \phi_{150}\right)\right] \tag{3}$$

The total power in the ILS signal is denoted P_{GS}, and is $P_{GS} = A_c^2[1 + (D k_a)^2]/2$.

For simplicity, we assume that the DS-SS signal is binary phase modulated (BPSK). We also assume coherent detection. The DS-SS signal received by the aircraft can be defined as follows:

$$s(t) = \sqrt{2P}\, d(t)\, c(t) \cos\left(\omega_0 t + \theta\right) \tag{4}$$

where P is the signal power, $d(t)$ is the data modulation, $c(t)$ is the signal spreading code, ω_0 is the radian carrier frequency, and θ is the signal phase, which is assumed to be zero for convenience in our coherent receiver. The data waveform is

$$d(t) = \sum_k d_k\, p_T(t - kT) \tag{5}$$

where d_k is the kth bit, in $\{\pm 1\}$, T is the bit duration, and $p_x(t)$ is a unit amplitude rectangular pulse non-zero only in the interval $[0,x)$. The spreading signal is of a form similar to Eq. (5):

$$c(t) = \sum_{n=0}^{N-1} c_n\, p_{T_c}(t - nT_c) \tag{6}$$

with $c_n \in \{\pm 1\}$, T_c is the chip duration, equal to $1/R_c$, with R_c the chip rate, and the processing gain is $N = T/T_c$. As in most cellular systems, we assume the use of "long" spreading codes—codes whose period is much longer than a single bit. Hence, Eq. (6) represents a length-N subsequence of a much longer pseudo-random sequence. These long codes are well-modeled by random Bernoulli sequences.[11]

For the successful application of spectral overlay, the DS-SS bandwidth must be much larger than that of the GS signal. This bandwidth is proportional to the chip rate R_c. In Fig. 2 we illustrate conceptually the power spectrum of both signals in an overlay mode. This figure is for a single-carrier DS-SS signal, described by Eqs. (4-6). Multicarrier DS-SS signals may also be of interest; our work for the FAA and NASA is considering these signals, but for this paper we restrict attention to the single-carrier DS-SS case.
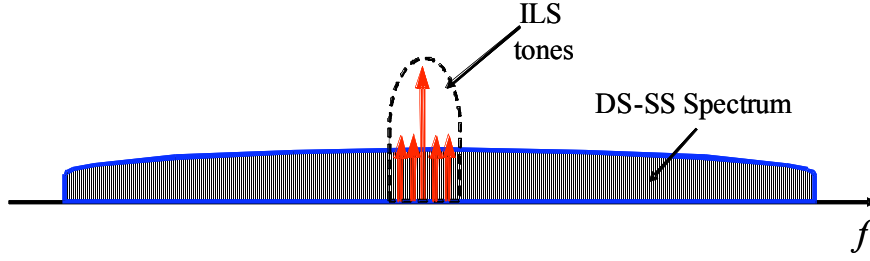
Fig. 2 Illustration of power spectrum of ILS with SC-DS-SS overlay.

III. Analysis

We are interested in quantifying the effect of the GS signal on DS-SS performance, and also the effect of the DS-SS signal on GS performance. For the digital DS-SS system, performance is measured by the bit error ratio (BER), and for the analog GS signal, we estimate the effective signal-to-noise ratio (SNR), more precisely, the signal-to-noise-plus-interference ratio (SNIR).

A. DS-SS Performance

In order to calculate the BER for the DS-SS system, it is necessary to first calculate the statistics of the output of the DS-SS receiver. Figure 3 shows a block diagram of the DS-SS receiver. In Fig. 3, $w(t)$ is the AWGN.
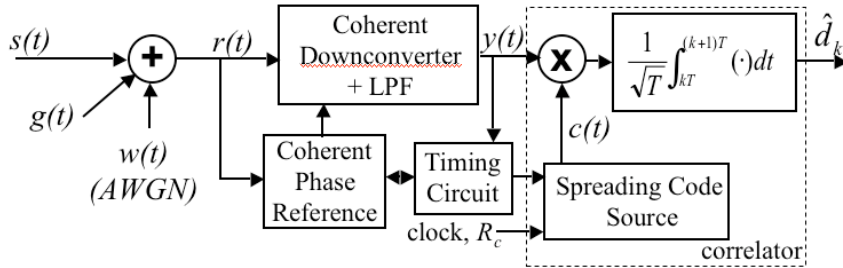

Fig. 3 Block diagram of a DS-SS receiver.

When the processing gain of the DS-SS signal is large, the effect of the GS signal can be modeled as an additive Gaussian disturbance to the desired signal. With this Gaussian approximation, we can obtain the BER in closed-form using standard functions. This relationship is illustrated in the following equation:

$$BER = P_b = Q\left(\sqrt{SNIR}\right) = Q\left(\sqrt{\frac{S}{N+I}}\right) \tag{7}$$

where S is mean-square value of the desired DS-SS part of the correlator output $\hat{d}_k$, N is the variance of the AWGN part, and I is the variance of the interfering GS signal part. The function $Q(x) = \frac{1}{\sqrt{2\pi}} \int_x^\infty e^{-t^2/2} dt$ is the tail integral of the zero-mean, unit-variance Gaussian probability density function. For coherent BPSK in AWGN only, the BER is given by the well known expression,[11] $P_b = Q\left(\sqrt{SNR}\right) = Q\left(\sqrt{2E_b/N_0}\right)$ where E_b is the received bit energy (equal to PT) and N_0 is the one-sided thermal noise power spectral density in W/Hz. To obtain the effect of the GS signal, we input $g(t)$ into the DS-SS receiver of Fig. 3, and calculate the variance of the DS-SS receiver output. The mean of the ILS part of $\hat{d}_k$ is zero when the spreading code is zero mean.

The first process performed by the receiver is down converting the GS signal and filtering out the double frequency components. This yields the following expression:

$$I(t) = \frac{A_c}{2}\left\{1 + Dk_a\left[\cos\left(2\pi 90t + \phi_{90}\right) + \cos\left(2\pi 150t + \phi_{150}\right)\right]\right\} \tag{8}$$

where $I(t)$ is the GS part of $y(t)$ in Fig. 3. We next multiply $I(t)$ by the spreading code, and integrate, over the bit period T, assuming without loss of generality that the integrator delay τ is zero. This yields the interfering GS part of the decision statistic $\hat{d}_k$, denoted I:

$$I = \sum_{n=0}^{N-1} c_n\left[\frac{A_c T_c}{2} + \frac{F}{2\pi 150}\left[\sin\left(2\pi 150T_c\left(n+1\right) + \phi_{150}\right) - \sin\left(2\pi 150nT_c + \phi_{150}\right)\right]\right.$$
$$\left. + \frac{F}{2\pi 90}\left[\sin\left(2\pi 90T_c\left(n+1\right) + \phi_{90}\right) - \sin\left(2\pi 90nT_c + \phi_{90}\right)\right]\right] \tag{9}$$

where $F=A_cDk_a/2$, and the other variables in Eq. (9) are as defined in the previous section. As noted, the mean of (9) is zero since the mean of the spreading code is assumed to be zero. To obtain the variance of Eq. (9), we square it and take the expected value of the resulting expression. Based upon the assumption of random spreading codes, after some trigonometry and algebraic simplification, this results in the following expression for the GS signal variance:

$$\sigma_I^2 = \frac{A_c^2 T_c^2}{4}\sum_{n=0}^{N-1}\left[1 + 2\beta S_1(T_c)C_1(n,T_c) + 2\beta S_2(T_c)C_2(n,T_c)\right.$$
$$\left. + 2\beta^2 S_1(T_c)S_2(T_c)C_1(n,T_c)C_2(n,T_c) + \beta^2 S_1^2(T_c)C_1^2(n,T_c) + \beta^2 S_2^2(T_c)C_2^2(n,T_c)\right] \tag{10}$$

where we have defined $\beta=Dk_a$, $S_1(T_c) = sin(\pi 150T_c)/(\pi 150T_c)$, $S_2(T_c) = sin(\pi 90T_c)/(\pi 90T_c)$, $C_1(n,T_c) = cos[\pi 150T_c(2n+1)+\varphi_{150}]$, and $C_2(n,T_c) = cos\ [\pi 90T_c(2n+1)+\varphi_{90}]$.

Using Eq. (10), we can obtain the following expression for error probability for the DS-SS system in the presence of the GS signal:

$$P_b = Q\left(\sqrt{\frac{2E_b}{N_0 + 4\sigma_I^2/T}}\right) \tag{11}$$

In addition, for rapid evaluation, we have the following bounds on the GS term variance, obtained by setting the sinusoidal terms defined after Eq. (10) to plus or minus unity:

$$\sigma_I^2 \leq \frac{A_c^2 T_c^2}{4}N[1+2\beta]^2 \tag{12}$$

$$\sigma_I^2 \geq \frac{A_c^2 T_c^2}{4}N[1-2\beta]^2 \tag{13}$$

These terms can be used in Eq. (11) to provide bounds to DS-SS error probability performance. When $\beta=0$, $A_c^2/2$ is the total GS glideslope transmitted power, and we have the case of a single tone interferer, as studied in Ref. 11.

B. GS Performance

For assessing the degradation incurred by the GS system in the presence of the DS-SS signal, we model the DS-SS interference as wideband, white Gaussian noise. Hence, the GS "noise" increases from P_N to P_N+I_{DS}, where $P_N = N_0B_{GS}$ is the AWGN thermal noise power within the GS receiver band B_{GS}, and I_{DS} is the DS-SS interference signal power in that same band. The exact value for the GS receiver bandwidth may depend upon the receiver manufacturer, but given this bandwidth, it is simple to obtain the value for I_{DS}: for a GS receiver bandwidth of B_{GS},

we have $I_{DS} \cong P(B_{GS}/R_c)$. Hence for any given value of bandwidth and received DS-SS power, we can easily compute the value of the GS SNIR.

$$SNIR_{GS} = \frac{P_{GS}}{P_N + PB_{GS}/R_c} \qquad (14)$$

As noted previously, while SNIR may not be the most important metric for assessing the DS-SS effect upon the ILS glideslope system, it is a reasonable one that is also analytically tractable. Exploration of better GS performance metrics is a subject for future work.

IV.   Numerical Results

We have computed the DS-SS BER according to Eq. (11) for several cases, to gain insight into the range of feasible values of several signal parameters. For simplicity, we assume the GS signal is 100% modulated, so that the carrier signal amplitude is twice that of the sideband amplitudes [Dk_a=1 in Eq. (3)]. This restriction is easily changed, and arbitrary parameter values can be used in Eq. (10). As noted, relative to the DS-SS signal, the phases and power levels of the GS signal will change depending upon spatial orientation as an aircraft approaches the GS transmitter; in this case DS-SS performance can still be ascertained via Eqs. (10) and (11) with appropriate parameter settings.

We have also developed computer simulations to corroborate the analytical results of the previous section. These simulations were conducted in MATLAB®. Parameters we can vary are the DS-SS processing gain N, the signal-to-noise (only) ratio, expressed as E_b/N_0, the ratio of the received GS signal power to the received DS-SS signal power, expressed as the jamming-to-signal-ratio (JSR), and the GS center frequency relative to the DS-SS center frequency.

We first show the effects of the GS signal upon the DS-SS performance. Figure 4 shows BER as a function of SNR for several different values of JSR. For simplicity in this plot, we have set all phases equal to zero, i.e., $\phi_{150}=\phi_{90}=0$. In Fig. 4, the chip rate of the DS-SS system is 5 MHz, and the bit rate of the DS-SS system is 5 kbps. These values yield a processing gain of 1000. If for example the DS-SS system requires an error probability of no greater than 10^{-3}, the acceptable JSR is approximately 10 dB—this can be translated, via link budget equations, into acceptable transmit power levels and ranges.
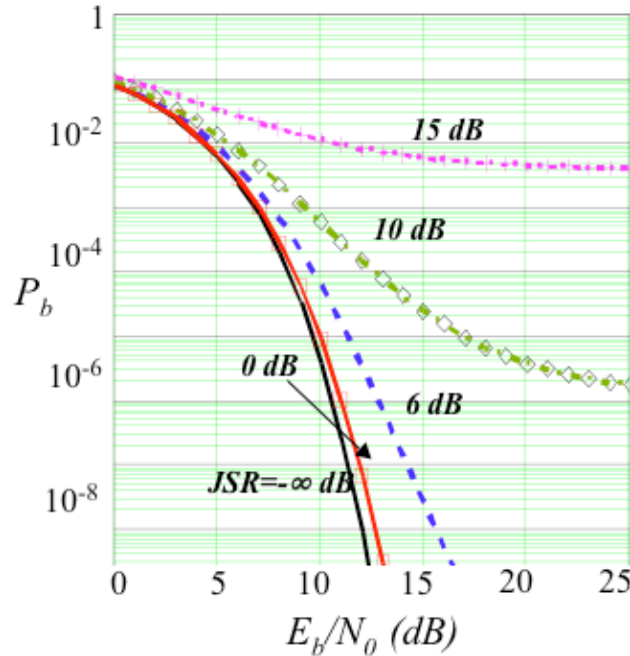

Fig. 4 DS-SS P_b vs SNR (E_b/N_0) with a processing gain of R_c/R_b=5MHz/5kbps=1000, for several values of JSR. Amplitudes of the GS sidebands are one-half that of the carrier, and all carrier phases are zero.

In Fig. 5, a plot similar to Fig. 4 is shown. In this case, the chip rate of the DS-SS system remains 5 MHz, but the bit rate is increased to 50 kbps. This results in a reduction of the processing gain from 1000 to 100. Notice the performance degradation from Fig. 4 to Fig. 5 for identical JSR values. For example, for a DS-SS error probability of 10^{-3}, the maximum acceptable JSR in this case is only 0 dB. The higher data rate used in Fig. 5 requires a smaller JSR for the same DS-SS performance. We also show the effect of the tone phases. Specifically, all curves other than the AWGN (JSR= $-\infty$ dB) and the 0 dB JSR curve use a JSR=10 dB, and the tone phases are specified by the vector $\Phi=[\phi150, \phi90]$. The enormous effect of these carrier phases is evident. We have also plotted the performance using the upper bound of Eq. (12) for JSR=10 dB. This plot is coincident with the one for $\Phi=[0, 0]$.
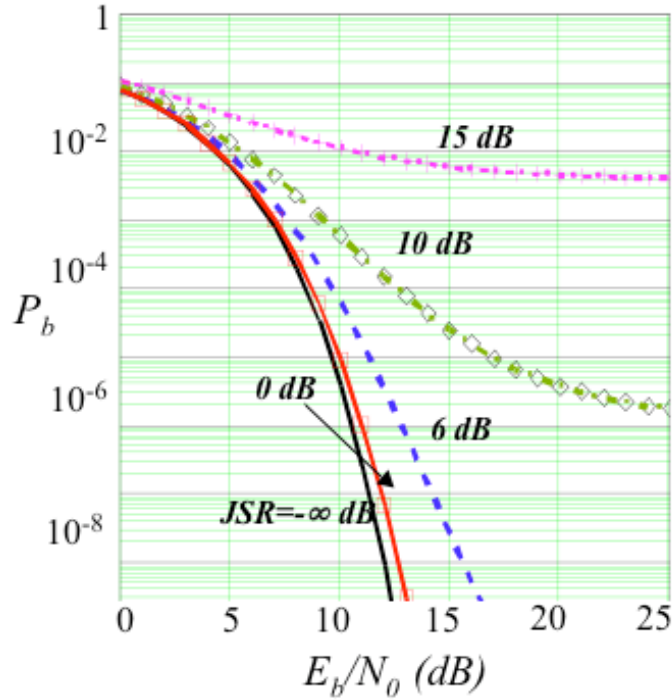

Fig. 5 DS-SS P_b vs SNR (E_b/N_0) with a processing gain of R_c/R_b=5MHz/50kbps=100 for several values of JSR ($-\infty$, 0, and 10 dB). Amplitudes of the GS sidebands are one-half that of the carrier, and carrier phases are specified by the vector $\Phi=[\phi_{150}, \phi_{90}]$.
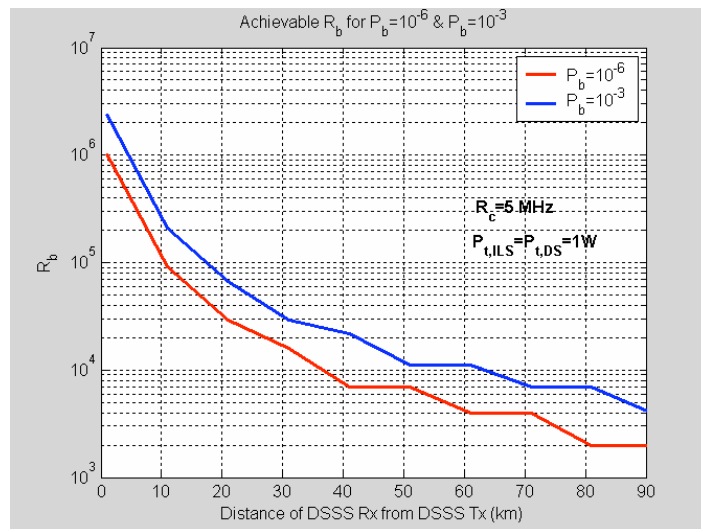

Fig. 6 Achievable DS-SS data rate R_b (bps) for a given P_b vs link range, in presence of GS.

In Fig. 6, the achievable bit rate for two DS-SS systems in the presence of the GS interference is plotted as a function of distance between the DS-SS receiver and DS-SS transmitter (i.e., communication link range). As with the previous plots, the GS sideband amplitudes are one-half that of the carrier, and in this case, the phase vector is $\Phi = [\phi_{150}, \phi_{90}] = [\pi, 0]$. A desired value for BER is assumed for each system, which translates into a fixed value for the DS-SS SNIR in Eq. (11). It is also assumed that the distance between the DS-SS receiver and DS-SS transmitter is identical to that between the GS transmitter and GS receiver, or in other words, the DS-SS and GS ground transmitters are close compared to the link range. In addition, we assume that both the GS and DS-SS transmitters transmit one watt of power (hence JSR=0 dB). Finally, a chip rate of 5 MHz is assumed for both systems. Figure 6 was obtained numerically, based upon simple link equations, in which all antenna gains are zero dB, the channel attenuation is modeled as that of free space, and receiver noise figures are 10 dB. Worth noting is the fact that these results apply to uncoded modulation—actual error probabilities would be significantly lower with forward error correction, which would be used in any practical system.

In Fig. 7, we compare the DS-SS analytical P_b results to those of our simulation. For these plots we used the "artificial" condition of 200% modulation, yielding equal amplitudes for all tones, solely for simplicity and validation of our analysis. Excellent agreement is obtained. The real utility of simulations would be for cases where the analysis becomes intractable, e.g., for random initial spatial orientation and tone phases, varying in time and space.

For the GS SNIR in the presence of the DS-SS signal, we show in Fig. 8 the achievable GS SNIR versus the DS-SS bandwidth, for five different values of GS receiver bandwidth, 300 Hz, 1 kHz, 5 kHz, 10 kHz, and 100 kHz. The SNR (without any DS-SS signal present) is 10 dB, and the JSR is zero dB. Clearly, the lower the value of GS receiver bandwidth and the larger the DS-SS bandwidth, the higher the resulting GS SNIR.
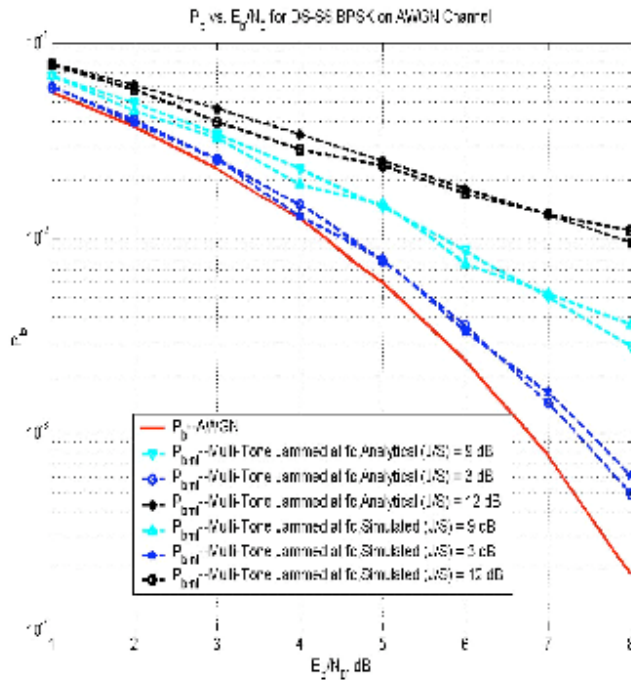

Fig. 7 P_b vs E_b/N_0 for DS-SS in presence of GS; analytical and simulation results. Amplitudes of the GS sidebands are equal to that of the carrier, and all GS tone phases are zero.
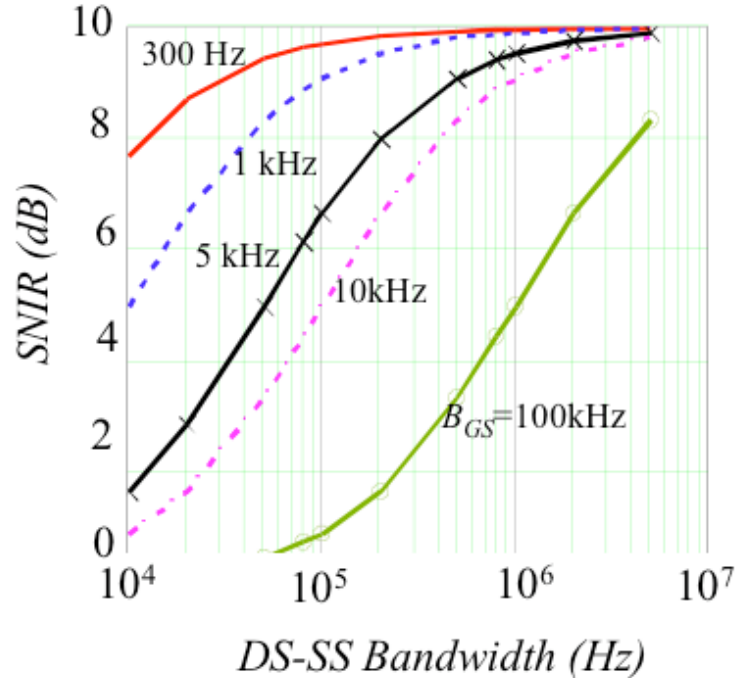
Fig. 8 GS SNIR vs DS-SS bandwidth, with five GS receiver bandwidths B_{GS}: 300 Hz, 1 kHz, 5 kHz, 10 kHz, and 100 kHz. GS SNR=10 dB, and JSR=P_{DS}/P_{GS}=0 dB.

V. Summary and Conclusions

In this paper, we have explored the feasibility of the use of spectral overlay of DS-SS in the ILS glideslope band, for a potential new digital data link. Using classical analytical techniques and a first-order model for the channel, we developed expressions for the error probability performance of DS-SS in the presence of GS interference, and for the signal-to-noise ratio performance of GS in the presence of DS-SS. We corroborated our analytical results with computer simulations.

We identified the pertinent DS-SS signal parameters necessary for a proper evaluation: the DS-SS processing gain and data rate, and the transmit power. The GS signal/system parameters of most importance are the GS signal power and receiver bandwidth; spatial variation of the GS signal is also very important, and accounting for this is a subject for future work. Given a careful system design, and allowing either some small degradation to the GS received SNR, or a slightly reduced GS range, the use of a DS-SS spectral overlay is feasible.

Our results are the first of those required for a proper application of spectral overlay, and serve to illustrate the method. Additional work is required to firmly establish the feasibility of this technique. This work would begin with obtaining accurate values of the GS receiver bandwidth, and minimally acceptable values of the GS SNR, in addition to accounting for spatial effects. The use of realistic link ranges would also be needed to estimate potential performance and data rates of the DS-SS system. Other areas of research include the use of interference canceling (filtering) of the GS signal in the DS-SS receiver to improve DS-SS performance, and filtering the DS-SS transmissions (spectral "notching") to improve GS performance.[12] Finally, the use of multiple-carrier DS-SS signals should be explored.[13] The use of this signal type could remove the need for filtering that might be required in a single-carrier DS system.

References

[1]Department of Transportation, Federal Aviation Administration National Airspace System Web site, http://www2.faa.gov/nasarchitecture/blueprnt/comm.htm, 27 June 2003 (cited Oct. 2004).

[2]Burke, G., "Shaping the National Airspace System for the 21st Century," *Proceedings of the 16th Digital Avionics Systems Conference*, 26-30 Oct. 1997, pp. 0.4-1—0.4-7.

[3]Smith, P., "IPSKY: IPv6 for the Aeronautical Telecommunications Network," *Proceedings of the 20th Digital Avionics Systems Conference*, 14-18 Oct. 2001, pp. 7.A.6-1—7.A.6-11.

[4]Martzaklis, K., "NASA Datalink Communications Research & Technology Development For Aeronautics," *Proceedings of Integrated CNS Workshop, Session E—Research and Technology Development for Far-Term Datalink Systems*, 1-3 May 2001.

[5]Kabaservice, T. P., "Technical and Economic Benefits of VHF Digital Link Mode 3 Integrated Voice and Data Link for Air Traffic Control Communications," *Proceedings of the Integrated CNS Workshop, Session B1—Datalink Communication Systems*, 19-22 May 2003, pp. 55-59.

[6]Jahn, A., Holzbock, M., Muller, J., Kebel, R., de Sanctis, M., Rogoyski, A., Trachtman, E., Franzrahe, O., Werner, M., Hu, F., "Evolution of Aeronautical Communications for Personal and Multimedia Services," *IEEE Communications Magazine*, Vol. 41, No. 7, July 2003, pp. 36-43.

[7]Matolak, D. W., "CDMA for Communications in the Aeronautical Environment," *Proceedings of the 16th Digital Avionics Systems Conference*, Oct. 1997, pp. 9.4-21—9.4-28.

[8]Haas, E., Schnell, M., "Advanced Airport Data Link—Concept and Demonstrator Implementation for a Modern Airport Data Link," *Proceedings of the Integrated CNS Workshop, Session B1—Datalink Communication Systems*, 19-22 May 2003, pp. 83-92.

[9]Milstein, L. B., Schilling, D. L., Pickholtz, R. L., Kullback, M., Kanterakis, E. G., Fishman, D. S., Biederman, W. H., and Salerno, D. C., "On the Feasibility of a CDMA Overlay for Personal Communications Networks," *IEEE Journal Selected Areas in Communications*, Vol. 10, May 1992, pp. 655-668.

[10]Helfrick, A., *Principles of Avionics*, 3rd ed., Avionics Communications, Inc., 2004.

[11]Peterson, R. L., Ziemer, R. E., and Borth, D. E., *Introduction to Spread Spectrum Communications*, Prentice-Hall, Upper Saddle River, NJ, 1995.

[12]Matolak, D. W., "On the Overlay of CDMA onto the Aeronautical VHF Band: An Inter-System Interference Analysis," MITRE Technical Report 97W0000137, Dec. 1997.

[13]Kondo, S., and Milstein, L. B. "Performance of Multicarrier DS CDMA Systems," *IEEE Transaction Communications*, Vol. 44, No. 2, Feb. 1996, pp. 238-246.